ELSEVIER

Journal of Alloys and Compounds 218 (1995) 143–148

Journal of ALLOYS AND COMPOUNDS

Solubility of Ti with C in the $Nd_2Fe_{14}B$ system and controlled carbide precipitation

D.J. Branagan, R.W. McCallum

Ames Laboratory, USDOE, and Department of Material Science and Engineering, Iowa State University, Ames, IA 50011, USA

Received 11 August 1994; in final form 22 August 1994

Abstract

An investigation has been launched to understand the unique solubility of titanium with carbon in the $Nd_2Fe_{14}B$ system. In order to restrict grain growth effectively, a stable dispersion of many fine precipitates must be formed. In order to form an effective dispersion, the solubilities of the precipitating elements should be understood. This includes the liquid and solid solubilities as well as the equilibrium and non-equilibrium solubilities. Samples made by ingot casting and melt-spinning were examined. The solubility limit of titanium and carbon in the liquid phase was found to be between 4 and 6 at.% Ti+C. Once the solubility limit of the liquid is exceeded, primary TiC precipitates form in the liquid at high temperatures. The maximum solid solubility in the 2-14-1 phase depends on the existence of other phases and is found to be cooling-rate-dependent. For TiC, the solid solubility is found to equal the liquid solubility. The cooling-rate dependence indicates that the titanium and carbon exist in supersaturated solid solution. The equilibrium solubility in the 2-14-1 phase is found to be less than or equal to 0.06 wt.% Ti. Owing to its favorable solubility, TiC is found to be an exemplary alloying addition in the $Nd_2Fe_{14}B$ system, and can be used to alter beneficially the extrinsic properties of the microstructure while maintaining the excellent intrinsic properties of the hard magnetic phase.

Keywords: Annealing; Crystallization; Magnetic properties; Microstructure

1. Introduction

$Nd_2Fe_{14}B$ (2-14-1) has proven to be an economically important permanent magnet material. It has extremely high intrinsic magnetic properties, with a theoretical energy product of 64 MG Oe [1]. In bulk permanent magnets, the extrinsic properties relating to the microstructure determine the level of hard magnetic properties that is actually achieved. Many researchers have worked on the microstructure property relationships in the 2-14-1 system [2–6]. For rapidly solidified material, the coercivity has been found to be very intricately tied to the grain size of the hard magnetic phase [7–8]. Theoretically the optimum grain sizes are between 50 and 100 nm [9], which is below the single-domain particle limit of grains [10]. While such fine grain sizes are easily obtained during rapid solidification, densification of these materials without excessive grain growth is difficult. Recently it has been shown that the addition of refractory-metal carbides to the melt results in both more uniform nucleation when crystallizing a glass precursor and better stability of the magnetic properties during anneals above the plastic deformation temperature, which should relax the processing conditions for densification of the materials [11].

Enhanced high-temperature stability of the microstructure of the 2-14-1 material results from the grain boundary pinning effects of precipitates. To prevent grain growth effectively, a fine dispersion of precipitates must be formed, since the maximum pinning force for grain boundaries from precipitates increases as the volume fraction of precipitates increases and as the size of the precipitates decreases [12]. Previous studies have shown that in the Nd–Fe–B–Ti system, the most stable phases are TiB_2 and Nd_2Fe_{17} [13]. However, in the Nd–Fe–B–Ti–C system, the balance of free energies leading to equilibrium phase formation allows $Nd_2Fe_{14}B$ and TiC to be the most stable phases, and no titanium boride phases are found [13].

In this paper, the equilibrium and non-equilibrium solubilities of Ti with C in the liquid and solid phases will be examined in detail in order to understand the precipitation process better. To meet these goals, ingot-cast and melt-spun samples were examined. The scale of the microstructure is much finer and is much more difficult to study in melt-spun samples compared to the

SSDI 0925-8388(94)01393-4

as-cast samples. However, the alloy chemistry depends on the balance of free energies and should be similar in both types of samples. In this paper, transmission electron microscopy was not done. The solubilities in the ingot material could be determined in a direct fashion through scanning electron microscopy (SEM) and the solubilities of the melt-spun material could be related in an indirect fashion through studying changes in properties. Also, since the cooling rate varies greatly (about 10^3 °C s^{-1}) between the two types of samples, any cooling-rate dependence of solid solubility can be deduced.

2. Experimental procedure

Starting ingots for all alloys used in this study were prepared from the elements by arc-melting in ultra-high-purity Ar (UHPAr) gettered by a Zr button from high-purity elements (99.99 wt.% Fe, 99.95 wt.% Nd, 99.95 wt.% B, 99.97 wt.% Ti, and spectrographic grade C). Samples were melted and turned at least four times to insure homogeneity. The compositions of the alloys studied are shown in Table 1. Compositions are given in the form $(Nd_{2/17}Fe_{14/17}B_{1/17})_{100-2x}+Ti_xC_x$. Melt-spinning was done at ambient pressure in UHPAr. A quartz crucible with a 0.8 mm orifice was used. Solidification occurred on a copper wheel. The melt-spinning ejection temperature was 1375 °C. The orifice-to-wheel distance was 5 mm. Heat treating was done by wrapping the as-spun ribbon in tantalum foil. The foil packets were then sealed in quartz tubes with UHPAr at 0.5 atm. The heat treatment of melt-spun ribbons was done in a furnace calibrated with a NIST-traceable standard thermocouple.

X-Ray diffraction was performed on ribbons powdered under N_2 with Cu Kα radiation on a Philips X-ray Diffractometer. Differential thermal analysis (DTA) was performed with a Perkin–Elmer DTA with a heating rate of 10 °C min^{-1} in UHPAr at a flow rate of 50 cm^3 min^{-1}. SEM was done on a Jeol JSM 6100 SEM with an Oxford Link Pentaset energy-dispersive spectrometer (EDS) detector. Semiquantitative analysis was achieved using a titanium standard with the appropriate ZAF (atomic number, absorbance and fluorescence) corrections on MICROPLUS software made by Dapple. Auger analysis was performed on a Perkin–Elmer 660 Scanning Auger Microprobe. Curie-temperature measurements were made on powdered samples with a Princeton Applied Research vibrating-sample magnetometer (VSM) at a field of 1 T. The VSM furnace temperatures were calibrated with a high-purity nickel standard.

Table 1
Composition of alloys studied

Alloy	Composition	Ti Add x	C Add x
2-14-1	$Nd_{2/17}Fe_{14/17}B_{1/17}$		
TiC ($x=0.5$)	$(Nd_{2/17}Fe_{14/17}B_{1/17})_{100-2x}+Ti_xC_x$	0.5	0.5
TiC ($x=0.75$)	$(Nd_{2/17}Fe_{14/17}B_{1/17})_{100-2x}+Ti_xC_x$	0.75	0.75
TiC ($x=1$)	$(Nd_{2/17}Fe_{14/17}B_{1/17})_{100-2x}+Ti_xC_x$	1	1
TiC ($x=2$)	$(Nd_{2/17}Fe_{14/17}B_{1/17})_{100-2x}+Ti_xC_x$	2	2
TiC ($x=3$)	$(Nd_{2/17}Fe_{14/17}B_{1/17})_{100-2x}+Ti_xC_x$	3	3
TiC ($x=4$)	$(Nd_{2/17}Fe_{14/17}B_{1/17})_{100-2x}+Ti_xC_x$	4	4
TiC ($x=5$)	$(Nd_{2/17}Fe_{14/17}B_{1/17})_{100-2x}+Ti_xC_x$	5	5
TiC ($x=6$)	$(Nd_{2/17}Fe_{14/17}B_{1/17})_{100-2x}+Ti_xC_x$	6	6
TiC ($x=7$)	$(Nd_{2/17}Fe_{14/17}B_{1/17})_{100-2x}+Ti_xC_x$	7	7

3. Results and discussion

3.1. Liquid solubility

In order to form an effective dispersion of precipitates to prevent grain growth, the precipitates should form out of supersaturated solid solution. In this way, a large number of fine dispersoids will form directly at the grain boundaries. To obtain an effective dispersion, the elements that form the precipitates must first have significant solubility in the liquid phase. The elements soluble in the liquid may then be soluble in the solid phase(s) that form upon solidification. Once the solubility limit of the liquid has been exceeded, primary precipitates will form in the liquid. The existence of carbides in high-temperature ferrous-based liquid is known in steel processing [14–15]. The primary precipitates are relatively large and are less effective at preventing grain growth, although they may have other significant effects [16].

3.1.1. As-solidified ingots

Initially, as-solidified arc-melted ingots were examined by SEM for TiC additions with $x=2,4,6$ to stoichiometric 2-14-1 [13]. In all cases the ingots consisted of 2-14-1 phase, properitectic Fe, and an unresolved rare-earth-rich eutectic phase probably consisting of α-Nd and $Nd_1Fe_4B_4$ phases. In the as-solidified arc-melted TiC ingot with $x=2$, no primary TiC precipitates were found. EDS analysis of the as-solidified phases indicated that Ti was homogeneously distributed in the 2-14-1 and Fe phases on the scale of the analysis, at levels of 1.30 wt.% and 1.71 wt.% respectively, for the $x=2$ addition. In the $x=4$ and $x=6$ TiC as-solidified alloys, primary TiC precipitates were present throughout the microstructure.

In Fig. 1, the as-cast TiC alloy with $x=4$ can be seen. The primary carbides have a cubic shape and are indicated by the arrows. The equilibrium cubic shape of the carbides indicates that they formed first from the liquid. From EDS, the cubic precipitates were found to consist of only Ti and C. The X-ray diffraction

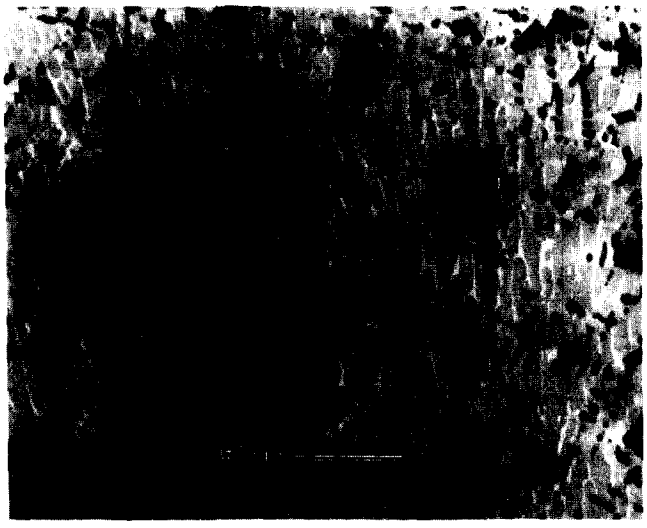

Fig. 1. SEM image of an as-cast TiC alloy with $x=4$. The primary TiC precipitates are marked with an arrow.

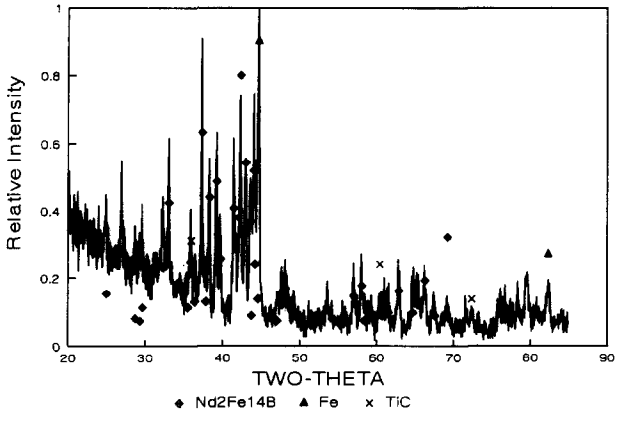

Fig. 2. XRD scan of the as-cast $x=4$ TiC-modified alloy.

scan of a powdered sample of the as-cast $x=4$ TiC alloy can be seen in Fig. 2. The X-ray diffraction scan verified that the cubic phase was TiC. Thus, for the rather undefined levels of superheat obtained during arc melting, the solubility of Ti with C in the liquid is found to be between 4 and 8 at.% Ti+C. Owing to the multiple meltings of the sample, it is expected that equilibrium was approximated in the melt, and the level of liquid solubility measured approximates the equilibrium solubility limit.

3.1.2. Melt-spun ribbon

In order to further verify that the blocky TiC precipitates did not form during solidification, melt-spun ribbons were studied. By melt-spinning at high wheel speeds (45 m s^{-1}), high cooling rates on the order of 10^6 °C s^{-1} are obtained, which causes the formation of a primarily amorphous or glassy structure [17]. This high cooling rate will not allow time for solid-state reactions requiring diffusion, such as TiC precipitation. An X-ray diffraction scan of a TiC alloy with $x=6$, melt-spun at 40 m s^{-1}, shows the presence of TiC in an amorphous matrix as shown in Fig. 3. In the X-ray scans, TiC was observed in the amorphous alloys at 8 at.% Ti+C and greater. X-Ray scans do not accurately indicate the limit of liquid solubility, owing to the poor detectability of the low-molecular-weight TiC precipitates. Auger analysis was done on an optimally quenched melt-spun TiC alloy with $x=6$. In the melt-spun alloy, primary TiC precipitates similar to those observed in as-cast ingots were found. These precipitates can be seen in Fig. 4. The existence of secondary carbides could not be verified owing to the resolution limit of the microscope, but additional titanium and carbon were found distributed homogenously throughout the matrix of the melt-spun ribbon.

While it is difficult to measure accurately the amount of Ti and C in solution in the amorphous phase, measuring the changes in the properties of this phase can give a good indication of the solubility limit. In Fig. 5, the crystallization temperature of the 2-14-1 phase is plotted vs. atomic percent Ti with C addition.

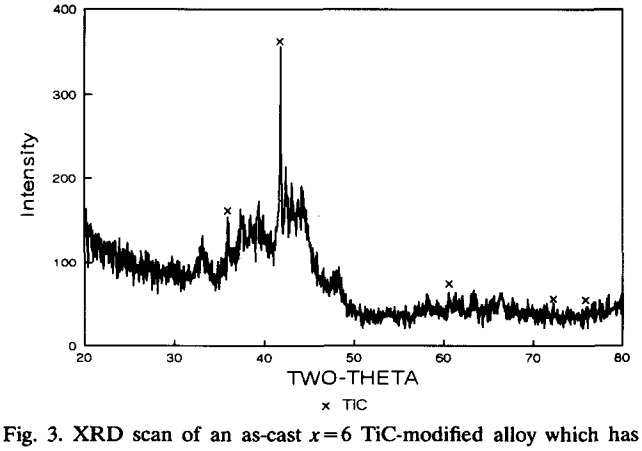

Fig. 3. XRD scan of an as-cast $x=6$ TiC-modified alloy which has been melt-spun at 25 m s^{-1}.

Fig. 4. Auger micrograph of a TiC-modified alloy with $x=6$, melt-spun at 10 m s^{-1}.

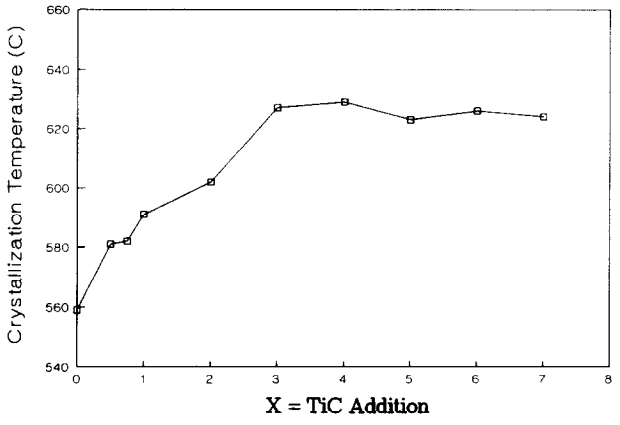

Fig. 5. Variation in crystallization temperature of the 2-14-1 phase with TiC addition.

It can be seen that between the $x=2$ and $x=3$ TiC alloys, the crystallization temperature reaches a plateau, and further additions of Ti and C do not increase the crystallization temperature. This plateau region supports the hypothesis that the solubility limit of Ti with C in the glass has been reached. Taken as a whole, the evidence strongly supports a maximum solubility of Ti with C in the liquid phase of between 4 and 6 at.% Ti + C.

3.2. Solid-phase solubility

While between 4 and 6 at.% Ti + C can be maintained in the liquid phase, the level of solubility in the 2-14-1 phase must be independently determined. It is important to know both the non-equilibrium and equilibrium solubilities of Ti and C in the 2-14-1 phase. At least non-equilibrium solubility is necessary because, to obtain an effective dispersion of precipitates, it is inherent that the precipitates form from supersaturated solid solution. This results in a fine and widely distributed array. The equilibrium solubility is important because any titanium or carbon left dissolved in the 2-14-1 phase will cause changes in the intrinsic magnetic properties.

3.2.1. 2-14-1-phase non-equilibrium solubility

Experiments were undertaken in both the arc-melted ingots and the melt-spun ribbons to find the maximum solubility of Ti with C in the 2-14-1 phase. In the arc-melted ingots, the level of Ti in the 2-14-1 phase was measured using EDS semiquantitative analysis. The amounts of Ti found in the 2-14-1 and α-Fe phases for the as-solidified arc-melted TiC alloys with $x=2$, 4 and 6 can be seen in Table 2. These results show that Ti has at least a 1.3 wt.% solubility in the 2-14-1 phase. This does not indicate the maximum solubility in this phase, owing to competition with the properitectic iron phase which exists in the as-cast ingots. From Table 2, at least 1.7 wt.% Ti is dissolved in the iron

Table 2
Semiquantitative analysis of wt.% Ti

Addition	x	α-Fe	2-14-1
TiC	2	1.71	1.30
TiC	4	1.15	0.64
TiC	6	1.76	1.24

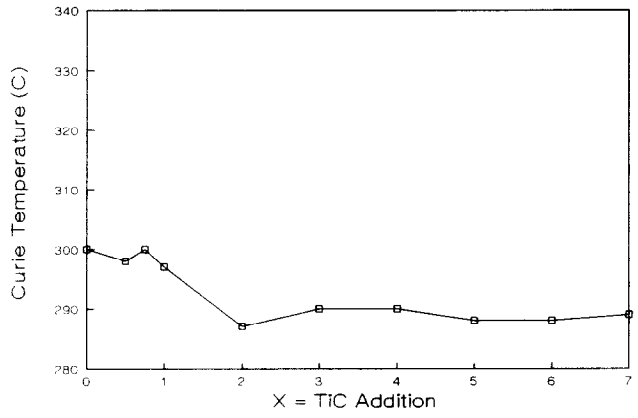

Fig. 6. Variation in Curie temperature with TiC addition for samples heat-treated at 650 °C for 1 h.

phase. In addition, during cooling and after solidification some titanium carbide precipitates are formed. This indicates that the titanium must exist in supersaturated solid solution. Through the study of the arc-melted ingots, titanium is found to have a significant solubility in the 2-14-1 phase.

Through melt-spinning at high wheel speeds, the peritectic and eutectic reactions can be avoided upon solidification, and a glassy or fine-grained 2-14-1 phase material can be formed directly. Owing to the extremely fine scale of the microstructure, changes in the physical properties as a function of alloy additions are used to detect elements in solution. Since it is known that C addition to the 2-14-1 phase lowers the Curie temperature [18], an amorphous phase was produced which after crystallization formed only the 2-14-1 phase, and the Curie temperature was determined. In Fig. 6, the Curie temperature vs. TiC addition can be seen for samples heat-treated at 650 °C for 1 h. From the figure it can be seen that the Curie temperature levels off between the $x=2$ and $x=3$ TiC alloys. This indicates that the solubility of Ti with C is between 4 and 6 at.% Ti + C. This is concurrent with the liquid solubility, and shows that the Ti with C present in the liquid remains present in the 2-14-1 phase under rapidly solidified conditions. As shown from the ingot data, however, lower cooling rates allow time for some TiC precipitation during solidification. This is an indication that the solubilities as measured are non-equilibrium, and that the titanium with carbon exists in supersaturated solid solution.

3.2.2. 2-14-1-phase equilibrium solubility

To determine the equilibrium solubility, amorphous melt-spun samples were heat-treated at 800 °C for 8 h. Again the Curie temperature was used as a probe of the material. In Fig. 7, the Curie temperature is graphed vs. TiC addition. It can be seen that within experimental error a uniform Curie temperature is found, independent of composition. Also, the average Curie temperature of 312 °C is found, which is representative of the unalloyed stoichiometric $Nd_2Fe_{14}B$ phase [19]. These data indicate that, after the 800 °C heat treatment, most or all of the Ti and C precipitated out of supersaturated solid solution.

As an added test, samples of arc-melted ingots were homogenized at 1000 °C for one week. During the homogenization heat treatment, many fine TiC acicular-shaped precipitates from 0.5 to 1.0 μm long were formed in the microstructures of the TiC alloys with $x=2$, 4 and 6. The primary (labeled 1) and secondary (labeled 2) precipitates can be seen in the $x=4$ TiC homogenized alloy in Fig. 8A. This composite microstructure is found to consist of only two phases. X-Ray diffraction scans verify that the phases observed are 2-14-1 and TiC. In Fig. 8B, it can be seen that many of these precipitates formed on the properitectic iron dendrites, which then subsequently reacted with the rare-earth eutectic to form additional 2-14-1 phase. Note that in the melt-spun ribbon there is no free iron present, and the TiC precipitates will use the grain boundaries as sites for heterogeneous nucleation.

EDS was performed on the matrix 2-14-1 phase after the homogenization heat treatment. The measured solubilities after homogenization are shown in Table 3. Thus, the equilibrium solubilities are found to be less than or equal to 0.06 wt.% Ti in either the $x=2$, 4 or 6 TiC homogenized alloys. The equilibrium solubility may be less, owing to the formation of the many precipitates in the microstructure. Owing to the spot size and interaction volume of the electron beam, it is very difficult to find an area without carbide influence.

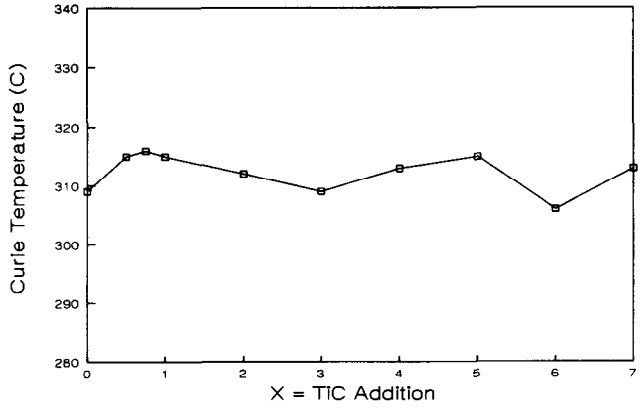

Fig. 7. Variation in Curie temperature with TiC addition for samples heat-treated at 800 °C for 8 h.

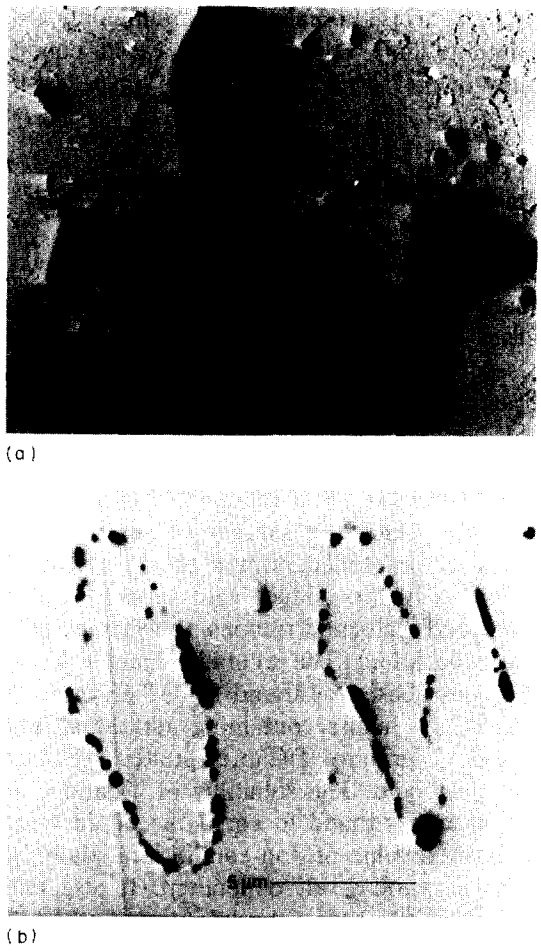

Fig. 8. SEM images of a TiC alloy with $x=4$, homogenized at 1000 °C for one week. (A) The primary and secondary TiC precipitates are labeled 1 and 2 respectively. (B) The secondary carbides trace out the prior iron dendritic boundaries which have since homogenized.

Table 3
Semiquantitative analysis of wt.% Ti

Alloy	x	2-14-1
TiC	2	0.06
TiC	4	0.00
TiC	6	0.02

Nevertheless, the loss of Ti and C from the 2-14-1 phase indicates that the equilibrium solubility of Ti with C in the 2-14-1 phase is very low.

It should be noted that these results are in contrast to those of Ti alone. Owing to TiC's extremely high free energy of formation (180.438 kJ mol^{-1}) [20], C essentially pulls the Ti out of solid solution and causes the formation of the TiC. If Ti is added alone to stoichiometric 2-14-1, Ti borides will form. In this case, however, there is a competition between using the boron to form the Ti boride and using the boron to form the 2-14-1 phase. This results in an equilibrium where some of the Ti remains dissolved in solid solution.

In stoichiometric 2-14-1 alloys containing only Ti below the solubility limit, Ti is found to have an equilibrium solubility of 0.47 wt.% in the 2-14-1 phase [13].

4. Summary

The maximum precipitate pinning force at the grain boundaries increases as the size of the precipitates decreases and as the volume fraction of precipitates increases. In order to restrict grain growth effectively, a stable dispersion of many fine precipitates must be formed. The elements making up the precipitates should have significant solubility in the liquid phase. This may allow the elements to be retained in the solid during solidification. Once the solubility limit of the liquid phase has been exceeded, primary precipitates will form. From studies of arc-melted ingots and from studying overquenched melt-spun ribbons, the various solubility limits can be found. The solubility limit of Ti with C in the liquid phase was found to be between 4 and 6 at.% Ti+C. In alloys containing additional amounts of Ti and C, primary TiC precipitates are found to form in the liquid. The solubility of Ti and C in the 2-14-1 phase was found to equal the liquid solubility. The measured value of non-equilibrium solubility was found to be cooling-rate-dependent. It also depends on the competition between solubilities of other phases. In the arc-melted ingots, the observed solubility is less than the maximum, which is consistent with the multiphase microstructure and the lower cooling rate.

Ideally, the elements forming the precipitates should have no equilibrium solubility in the solid phase. From studies of melt-spun ribbons and arc-melted ingots, the equilibrium solubility of Ti with C in the 2-14-1 phase is found to be very low (not more than 0.06 wt.% Ti). Titanium carbide represents an exemplary addition which allows the extrinsic properties of the 2-14-1 phase to be altered and improved, while the excellent intrinsic properties of the 2-14-1 phase are maintained.

Acknowledgments

The authors wish to express their gratitude to K.W. Dennis and M.J. Kramer for their technical assistance and advice. Ames Laboratory is operated for the US Department of Energy by Iowa State University under contract No. W-7405-ENG-82. This investigation was supported by the Director of Energy Research, Office of Basic Sciences.

References

[1] J.J. Croat, *IEEE Trans. Mag., 25* (1989) 3550–3554.
[2] G.F. Zhou, X.K. Sun, S.Y. Fu, Y.C. Chuang, R. Grössinger and H.R. Kirchmayr, *Phys. Stat. Sol. (a), 120* (1990) 627–634.
[3] R. Ramesh and G. Thomas, *J. Appl. Phys., 67* (1990) 6968–6975.
[4] R.K. Mishra, *Mat. Res. Soc. Symp. Proc., 96* (1987) 83–92.
[5] M. Sagawa and S. Hirosawa, *J. Mater. Res., 3* (1988) 45–54.
[6] T.-Y. Chu and R.K. Mishra, *J. Appl. Phys., 69* (1991) 6046–6048.
[7] J.M. Elbicki, W.E. Wallace and V. Korablev, *IEEE Trans. Magn., 25* (1989) 3567–3571.
[8] R. Ramesh, G. Thomas and B.M. Ma, *J. Appl. Phys., 64* (1988) 6416–6422.
[9] F.E. Pinkerton, *Int. J. Powder Metall., 25* (1989) 29–35.
[10] K.D. Durst and H. Kronmuller, *J. Mag. Mag. Mater., 59* (1986) 86.
[11] D.J. Branagan and R.W. McCallum, to be published.
[12] T. Gladman, *JOM,* (1992) 21–24.
[13] D.J. Branagan and R.W. McCallum, to be published.
[14] G.F. Comstock, *Titanium in Iron and Steel*, The Engineering Foundation, New York, 1955.
[15] G.F. Comstock, *Titanium in Steel*, Pitman, New York, 1949.
[16] H. Sandberg, *Scand. J. Metall., 2* (1973) 233–241.
[17] J.J. Croat and J.F. Herbst, *MRS Bulletin,* (1988) 37–40.
[18] X. Feng and H.W. Wang, *J. Mag. Mag. Mater., 94* (1991) 49–52.
[19] A. Hütten, *JOM,* (1992) 11–15.
[20] D.R. Lide Jr., *Janaf Thermochemical Tables*, American Chemical Society and American Institute of Physics, 3rd edn., 1985, p. 14.